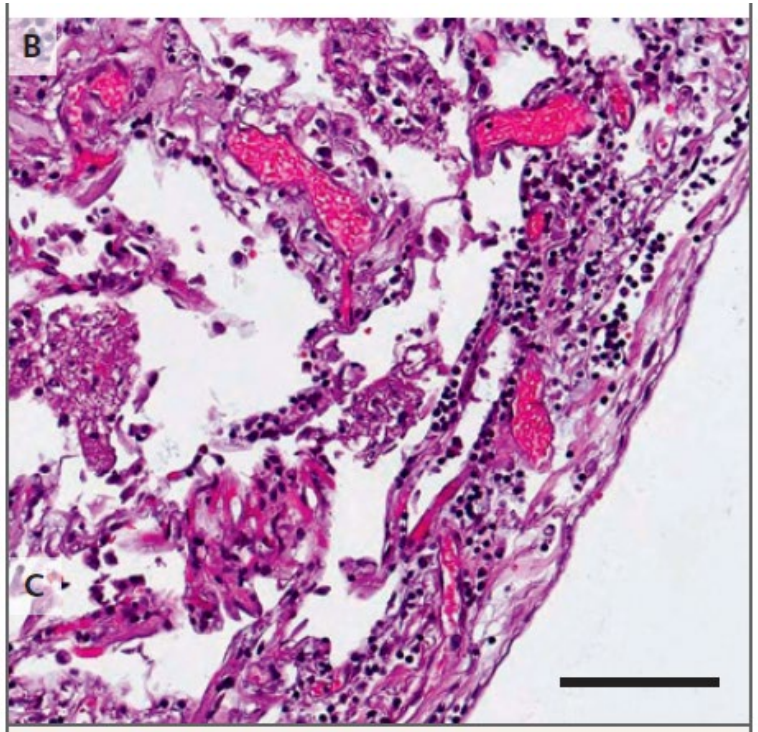

Figure 1. Lymphocytic Inflammation in a Lung from a Patient Who Died from Covid-19.

The gross appearance of a lung from a patient who died from coronavirus disease 2019 (Covid-19) is shown in Panel A (the scale bar corresponds to 1 cm). The histopathological examination, shown in Panel B, revealed interstitial and perivascular predominantly lymphocytic pneumonia with multifocal endothelialitis (hematoxylin–eosin staining; the scale bar corresponds to 200 μm).

- 細血管の壁は赤く変性しています。硝子様変性
- リンパ球の浸潤も多く認められます。

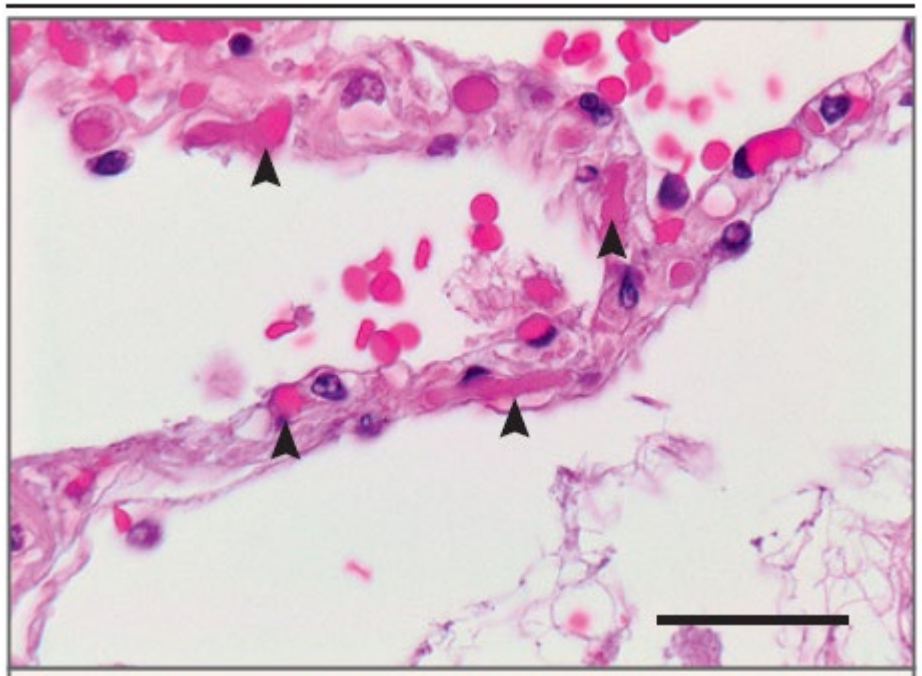

Figure 2. Microthrombi in the Interalveolar Septa of a Lung from a Patient Who Died from Covid-19.

The interalveolar septum of this patient (Patient 4 in Table S1A in the Supplementary Appendix) shows slightly expanded alveolar walls with multiple fibrinous microthrombi (arrowheads) in the alveolar capillaries. Extravasated erythrocytes and a loose network of fibrin can be seen in the intraalveolar space (hematoxylin–eosin staining; the scale bar corresponds to 50 μm).

- 肺胞壁の微小血管内に矢印の血栓が認められます。

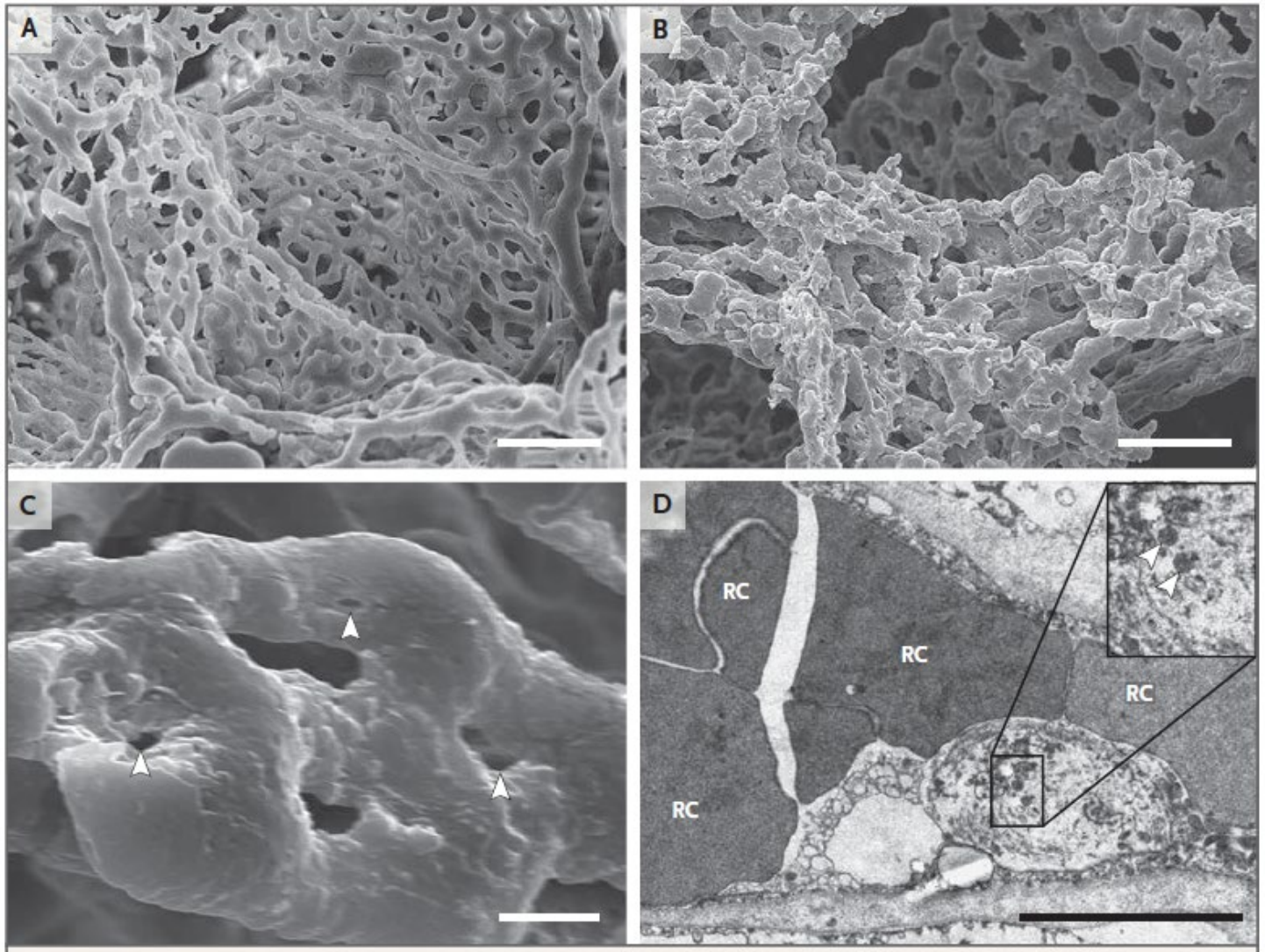

Figure 3. Microvascular Alterations in Lungs from Patients Who Died from Covid-19.

Panels A and B show scanning electron micrographs of microvascular corrosion casts from the thin-walled alveolar plexus of a healthy lung (Panel A) and the substantial architectural distortion seen in lungs injured by Covid-19 (Panel B). The loss of a clearly visible vessel hierarchy in the alveolar plexus is the result of new blood-vessel formation by intussusceptive angiogenesis. Panel C shows the intussusceptive pillar localizations (arrowheads) at higher magnification. Panel D is a transmission electron micrograph showing ultrastructural features of endothelial cell destruction and SARS-CoV-2 visible within the cell membrane (arrowheads) (the scale bar corresponds to 5 μm). RC denotes red cell.

- 走査顕微鏡です
- 肺胞の毛細血管の中に鋳型を作りそれを腐食して肺胞壁の微細なネットワークを見ています。

C図では血管内に隔壁が作られています。

・D図は普通の電子顕微鏡で肺胞の膜にコロナウイルスが存在しています。

血管新生の模式図です。

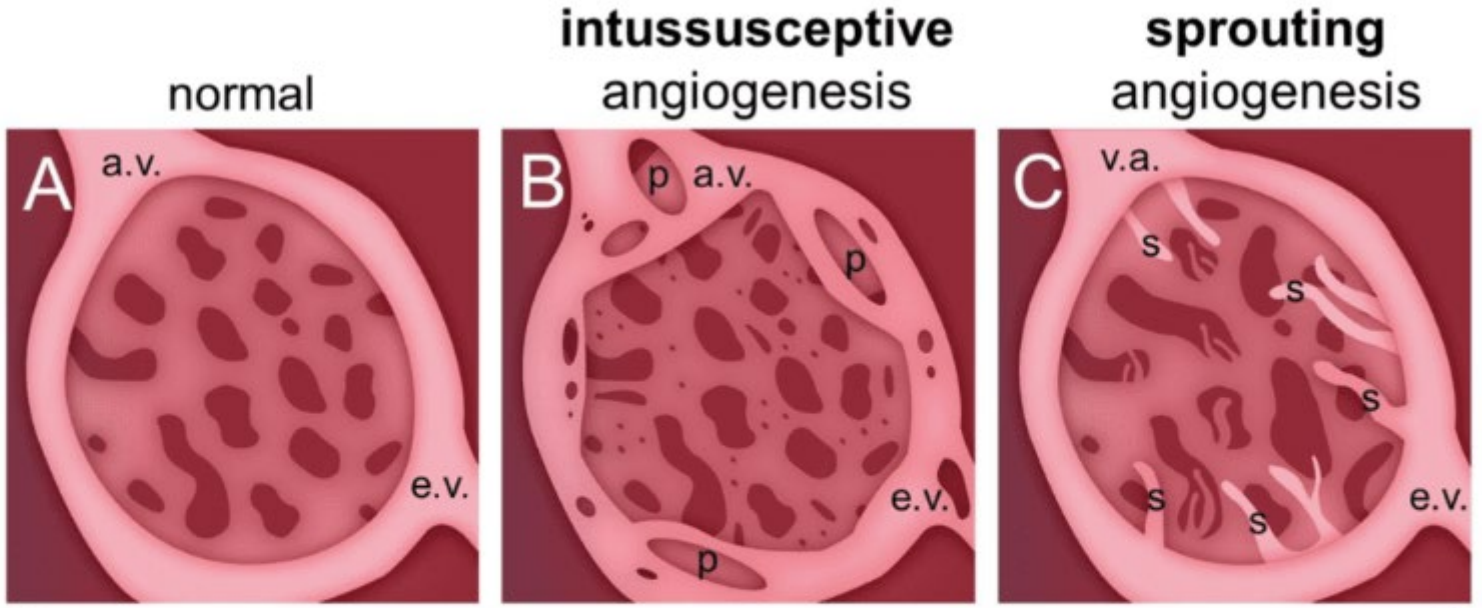
normal
intussusceptive
angiogenesis
sprouting
angiogenesis
A
a.v.
e.v.
B
p
a.v.
p
e.v.
p
C
v.a.
s
s
s
s
s
e.v.
A: Regular vasculature with afferent (a.v.) and efferent (e.v) vessels
B: Intussusceptive angiogenesis characterized by separation of preexisting blood vessels through the formation of an intravascular pillar (p)
C: Sprouting angiogenesis characterized by the formation of new channels (s) composed of endothelial cells from existing vessels

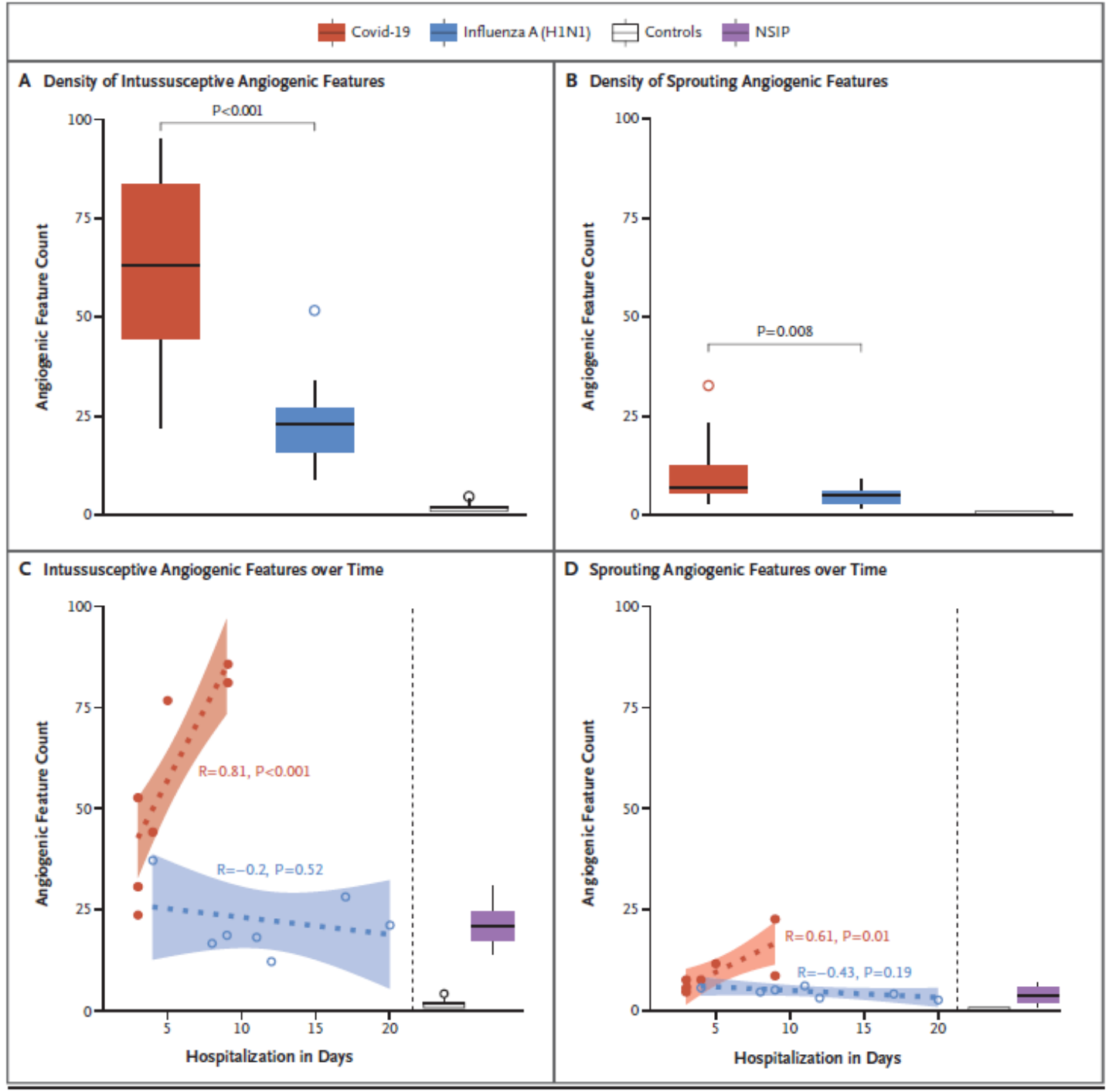
Covid-19
Influenza A (H1N1)
Controls
NSIP
A Density of Intussusceptive Angiogenic Features
P<0.001
Angiogenic Feature Count
100
75
50
25
0
B Density of Sprouting Angiogenic Features
P=0.008
Angiogenic Feature Count
C Intussusceptive Angiogenic Features over Time
R=0.81, P<0.001
R=−0.2, P=0.52
Angiogenic Feature Count
5
10
15
20
Hospitalization in Days
D Sprouting Angiogenic Features over Time
R=0.61, P=0.01
R=−0.43, P=0.19
Angiogenic Feature Count
Hospitalization in Days

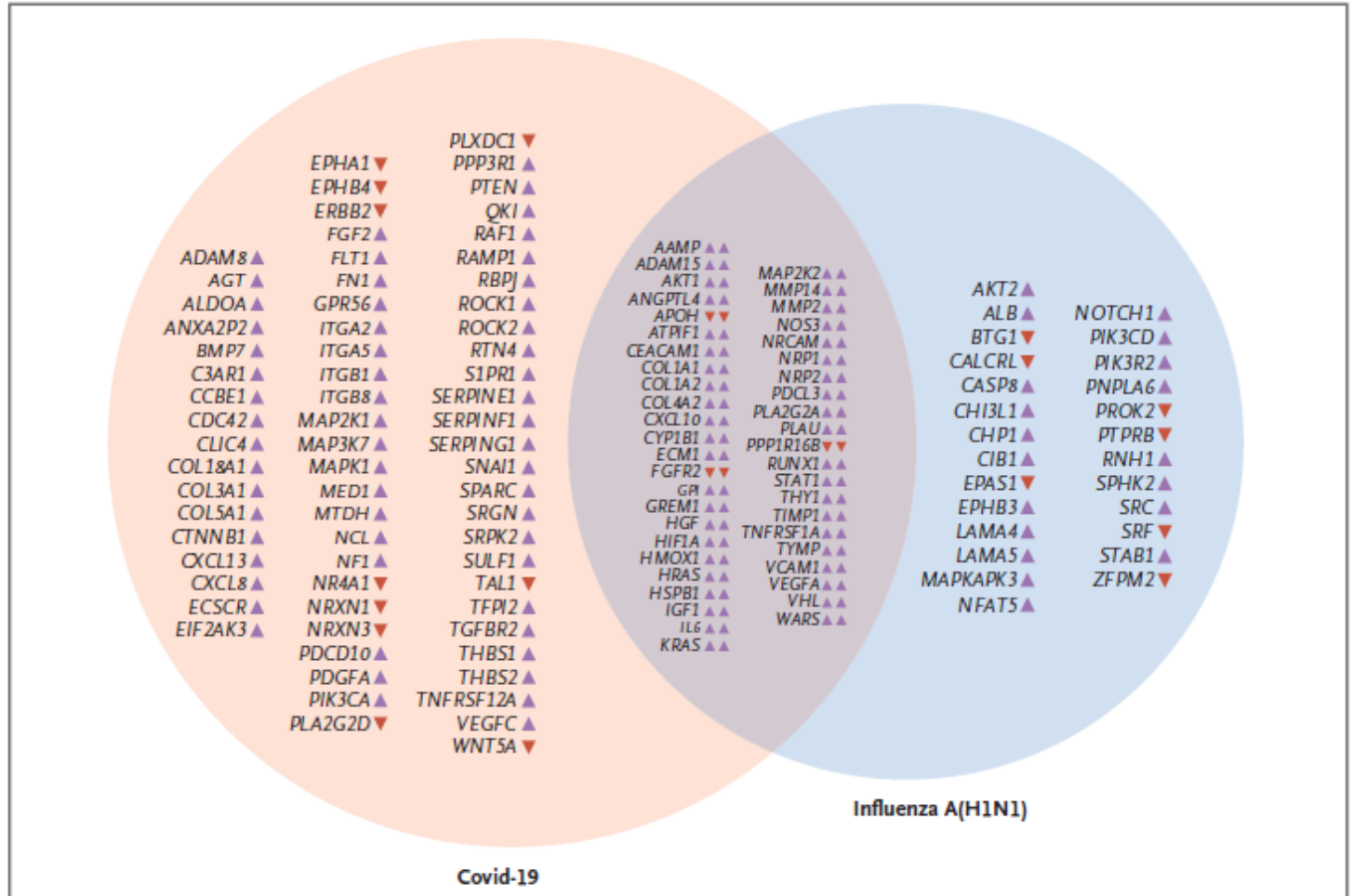

Figure 5. Relative Expression Analysis of Angiogenesis-Associated Genes in Lungs from Patients Who Died from Covid-19 or Influenza A(H1N1).

RNA was isolated from sections sampled directly adjacent to those used for complementary histologic and immunohistochemical analyses. RNA was isolated with the Maxwell RNA extraction system (Promega) and, after quality control through Qubit analysis (ThermoFisher), was used for further analysis. During the NanoString procedure, individual copies of all RNA molecules were labeled with gene-specific bar codes and counted individually with the nCounter Analysis System (NanoString Technologies). The expression of angiogenesis-associated genes was measured with the NanoString nCounter PanCancer Progression panel (323 target genes annotated as relevant for angiogenesis). The resulting gene-expression data were normalized to negative control lanes (arithmetic mean background subtraction), positive control lanes (geometric mean normalization factor), and all reference genes present on the panel (geometric mean normalization factor) with the use of nSolver Analysis Software, version 4.0. Shown in the Venn diagram are only genes that are statistically differentially expressed as compared with expression in controls in both disease groups (Student's t-test, controlled for the familywise error rate with a Benjamini–Hochberg false discovery rate threshold of 0.05). Up-regulation and down-regulation of genes is indicated by colored arrowheads suffixed to the gene symbols (purple denotes up-regulation, red denotes down-regulation).